JOURNAL OF PROPULSION AND POWER
Vol. 14, No. 5, September–October 1998

Atomization and Breakup of Cryogenic Propellants Under High-Pressure Subcritical and Supercritical Conditions

Wolfgang O. H. Mayer* and Axel H. A. Schik†
DLR, German Aerospace Center, Lampoldshausen, 74239 Hardthausen, Germany
Bruno Vielle,‡ Christian Chauveau,§ and Iskender Gökalp¶
Centre National de la Recherche Scientifique, 45071 Orleans Cedex 2, France
and
Douglas G. Talley** and Rodger D. Woodward††
U.S. Air Force Research Laboratory, Edwards Air Force Base, California 93524-7660

Recent results on the atomization and breakup of cryogenic propellants under high-pressure subcritical and supercritical conditions are surveyed. Cryogenic fluids were injected into various gases under both cold-flow and hot-fire conditions, and the results were visualized using flashlight photography and high-speed cinematography. In some cases, simulation fluids were used to study atomization and breakup behavior. In others, hot-fire tests with liquid oxygen and gaseous hydrogen demonstrated flow phenomena under realistic cryogenic rocket engine conditions. The visualizations reveal a remarkable difference between subcritical spray formation and evaporation and supercritical injection and mixing. As chamber pressure approaches the critical pressure, injection can no longer be regarded as simple "spray" formation, but rather as a fluid/fluid mixing process that can be extremely sensitive to small perturbations in pressure, temperature, local mixture concentrations, and initial injection conditions.

Introduction

CRYOGENIC rocket engines have evolved over the past 30 years and have been used in a number of operational launch vehicles wordwide. The thrust chamber is the core of any liquid rocket engine and consists of an array of injectors, a combustion chamber, and a nozzle. High performance and reusability are the most challenging requirements for future thrust chamber development, and will require large technical advancements for most of the engine components.[1]

Recent research into the injection, mixing, and combustion behavior of liquid oxygen/gaseous hydrogen (LOX/GH_2) propellants has provided an improved understanding of combustion processes in cryogenic rocket engine thrust chambers.[2–4] Despite this, many basic phenomena such as turbulent mixing still cannot be quantitatively predicted. The problem becomes increasingly severe at elevated chamber pressures. At pressures exceeding the critical points of the propellants, even qualitative understanding has often not been available.

In high-pressure liquid rocket engines, LOX can be injected at an initially subcritical temperature into an environment that exceeds the critical temperature and pressure of the oxygen. The LOX then undergoes a transition to a supercritical state as it is heated and burned. There are several reasons why such a process should be expected to be quite different than what is conventionally understood to occur under low-pressure, subcritical conditions.[5–8] These include the disappearance of surface tension, vanishing enthalpy of vaporization and other property singularities near the critical point, and enhanced solubility of the dispersed phase in the condensed phase. The latter reason creates mixture effects whereby the critical pressure of the mixture can reach several times the critical pressure of the pure component, depending on the environmental temperature. This in turn implies that instead of being fixed, the critical point can vary dynamically depending on the mixing, potentially causing the appearance or disappearance of gas/liquid interfaces. In addition, significantly reduced liquid/gas density ratios compared with conventional subcritical experience should cause comparatively stronger aerodynamic interactions, the magnitude of which should be even further enhanced as surface tension at the liquid interface is weakened.[9–11] Thus, turbulence interactions could play a more dominant role. The sum of all of these factors should affect the entire gamut of injection phenomena, from primary atomization, to secondary deformation and breakup, to "gasification," mixing, and combustion. For the sake of brevity, the term "transcritical" has often been used to refer to injection processes under conditions where the propellants can transform from a subcritical to a supercritical state, or vice versa, as a result of temperature, pressure, or mixture variations.

To better understand high-pressure subcritical and transcritical injection phenomena, several studies have been initiated by the authors. Recent progress is summarized later in this paper. The discussion begins with a hot-fire investigation of LOX/GH_2 injection under subcritical and supercritical conditions in a windowed combustion chamber. Cold-flow studies of jets where high-pressure subcritical and transcritical phenomena can be observed without the complications of chemical reactions are presented next. Finally, recent progress in studying the deformation and breakup of high-pressure subcritical and transcritical droplets is presented. The critical properties of relevant fluids are provided in Table 1.

Received Sept. 2, 1997; revision received May 11, 1998; accepted for publication May 18, 1998.

*Head of Propellant Injection Research, Rocket Propulsion. E-mail: wolfgang.mayer@dlr.de. Member AIAA.
†Research Engineer and Ph.D. Student, Rocket Propulsion.
‡Research Engineer and Ph.D. Student, Laboratoire de Combustion et Systèmes Réactifs.
§Scientist, Laboratoire de Combustion et Systèmes Réactifs.
¶Director of Research, Laboratoire de Combustion et Systèmes Réactifs.
**Group Leader, Rocket Combustion Devices, Propulsion Sciences and Advanced Concepts Division, 10 East Saturn Boulevard. Member AIAA.
††Scientist, 10 East Saturn Boulevard; currently Associate Director, Propulsion Engineering Research Center, Pennsylvania State University, University Park, 16802. Member AIAA.

Hot-Fire Jet Studies

Test Facility and Experimental Setup

An experimental rocket combustion chamber equipped with two flat windows for optical access was used to study injection and mixing under hot-fire subcritical and supercritical conditions.[3] The test rig consisted of an injector head with a single shear coaxial element, a circular, uncooled combustion chamber with a length and diameter of 400 and 40 mm, respectively, and a variable (exchangeable) nozzle (Fig. 1). The windowed section was cooled by a layer of GH_2, which was injected in the direction of the nozzle. Metal dummy windows with thermocouples were used to develop the startup and shutdown sequence and a suitable window-cooling technique. LOX was supplied to the test section from a helium- (He-) pressurized, vacuum-jacketed 90-m^3 storage tank. GH_2 to the injector and the window purge ports was supplied from a 20.0-MPa bottle depot. To cool the cryogenic supply line, a liquid nitrogen (LN_2) cooling jacket was installed between the LOX tank and the LOX dome. Chilling of the LOX line made it possible to reach steady-state firing conditions in less than 1 s. A small LOX/GH_2 pilot flame was used as the ignition source. The igniter was mounted on the lower part of the chamber wall. The typical duration of a firing was 5 s, including startup transients of approximately 0.1 s. A nontapered shear coaxial injector without recess was evaluated. The injector baseline dimensions were as follows: The outer diameter was 3.9 mm, the LOX post i.d. was 1 mm, and the LOX post tip-wall thickness was 0.3 mm. Further details may be found in Mayer and Tamura.[3]

Table 1 Critical properties of various fluids

	He	H_2	O_2	N_2	C_2H_6O
P_{cr}, MPa	0.231	1.307	5.081	3.42	6.38
T_{cr}, K	5.25	33.25	154.58	126.05	516

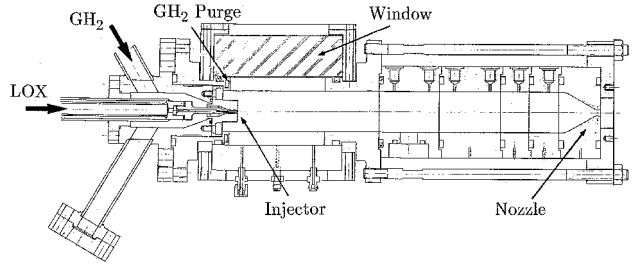

Fig. 1 Experimental LOX/GH_2 rocket combustion chamber with optical windows.

At low chamber pressures (2.0 MPa or less), flow-visualization studies were conducted with a standard camera and a flashlight in a shadowgraph and Schlieren setup. The typical shutter time was 1/60 s. A spark flashlight was used that had a typical pulse duration of less than 50 ns. The optical setup and filters were carefully selected and tested to determine the optimum between filtering propellant flame radiation and flashlight intensity losses.

The flame radiance increased dramatically at high chamber pressures. This required a special shadowgraph setup that included the need for a high-speed rotating disk shutter to be developed. The shutter speed was less than 1/1000 s. To filter the radiance of the flame an aperture was set between the combustion chamber and the camera lens. The light of the flash lamp was focused down to the aperture of the lens and was therefore not parallel. Thus, density gradients were visible when using this technique.

Test Conditions

The firing test conditions covered in this study were as follows: A chamber pressure of 1.0–10.0 MPa, an oxygen (O_2) injection velocity of 10–30 m/s, an O_2 injection temperature of 100 K, an H_2 injection velocity of 300 m/s, and an H_2 hydrogen injection temperature of 150–300 K.

Hot-fire tests with a nonrecessed coaxial injector at chamber pressures P_c of 1.5, 4.5, 6.0, and 10.0 MPa were conducted as described by test cases 1–4 in Table 2. The corresponding O_2 and H_2 velocities (u_{LOX}, u_{GH_2}) were 30 and 300 m/s, respectively, except for test case 1, where the LOX velocity was reduced to 10 m/s. This velocity reduction was necessary because the atomization and mixing efficiency at a chamber pressure of 1.5 MPa was so low that otherwise a large part of the LOX jet and ligaments would leave the chamber unburned and could not be visualized. The LOX temperature T_{LOX} was 100 K and the H_2 temperature T_{GH_2} was 300 K.

Results

Figure 2 shows shadowgraphs of the LOX jet taken at a subcritical pressure of 1.5 MPa (test case 1). At chamber pressures much less than the critical pressure of O_2, the LOX jet was atomized into a conventional spray. Following an initially

Table 2 Test case conditions

Test case	p_c, MPa	u_{LOX}, m/s	u_{GH_2}, m/s	T_{LOX}, K	T_{GH_2}, K
1	1.5	10	300	100	300
2	4.5	30	300	100	300
3	6.0	30	300	100	300
4	10.0	30	300	100	300

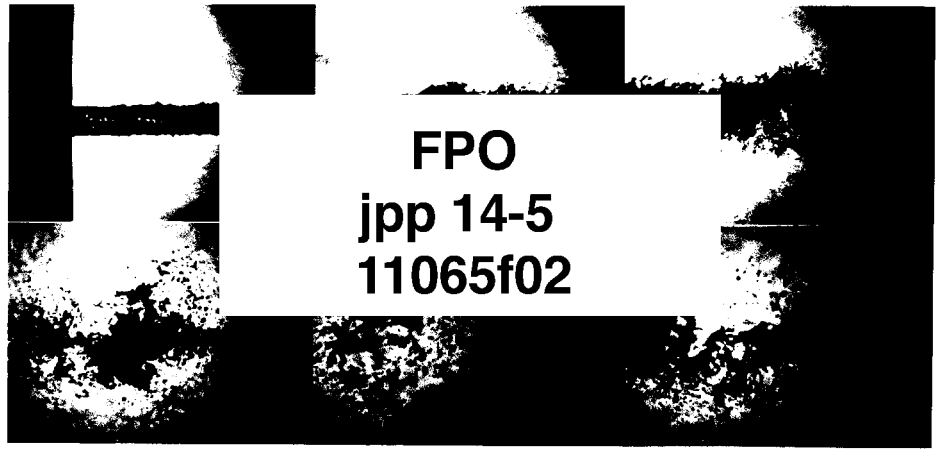

Fig. 2 Burning LOX jet at a subcritical pressure of 1.5 MPa (test case 1). Axial positions are x = 0 (faceplate), 12, 24, 36, 48, and 60 mm, from left to right and top to bottom.[3]

very smooth appearance of the jet surface close to the injector, ligaments formed and detached from the jet surface. These broke down into mostly nonspherical droplets that eventually evaporated. Secondary droplet breakup was also observed of the vibrational and bag types.

Figure 3 shows a comparison between cold-flow and hot-fire results that demonstrates the effect of the flame on the spray. The chamber pressure was the same as in Fig. 2: 1.5 MPa in both cases. Fine oxidizer ligaments and droplets were visible in the cold-flow, but not in hot-fire. The presence of the flame evidently vaporized such structures rapidly, leading to a significantly lower droplet number density. In fact, no droplets can be observed at all in the hot-fire visualization of Fig. 3. The smoothness of the round jet that can be seen in hot-fire can be attributed in part to rapid vaporization of the surface wave structures, but also to a considerable reduction in aerodynamic forces between the LOX jet and the H_2, because of the reduction in the density of all the gases in the 3500 K hot reaction zone.

Upon approaching and exceeding the critical pressure, distortion of the optical field by the surrounding coaxial flame increased. Careful interpretation of the results was required. Sample results are shown in Fig. 4 for a supercritical pressure of 6.0 MPa (test case 3). Despite the distortion, little evidence could be found that any droplets existed. Instead, stringy or thread-like structures developed and grew; they did not detach but rapidly dissolved and faded away. The LOX core broke up several tens of jet diameters downstream into large lumps that dissolved in the same manner. The average jet breakup length decreased with increasing chamber pressure. It may be noted that mixing and combustion was not yet complete at the farthest axial distance visualized in Fig. 4.

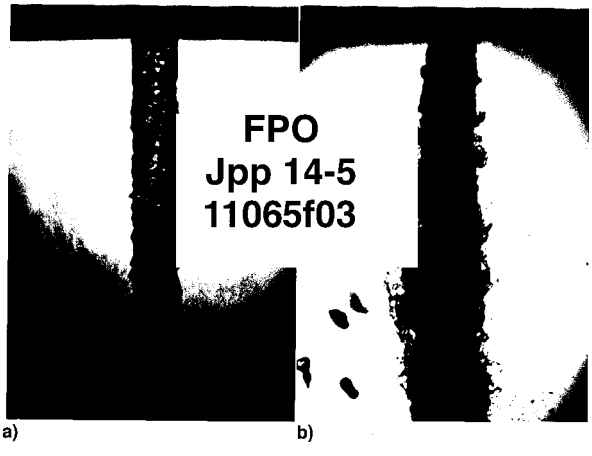

Fig. 3 Comparison of cold-flow and hot-fire visualizations at 1.5 MPa (test case 1): a) Burning after ignition and b) cold-flow before ignition.[3]

A very important result of this study was the observation of a LOX post wake flame and its interaction with the H_2/O_2 shear layer. This is illustrated in Fig. 5 for test case 2 (4.5 MPa). The photograph in Fig. 5a was taken with a standard shadowgraph setup and allows visualization of the LOX/hydrogen flame. To filter out the flame radiation, the photograph in Fig. 5b was taken by focusing the flash lamp through the lens aperture as described earlier, creating nonparallel rays allowing density gradients to be visible. The flame always attached instantaneously to the LOX post after ignition. A bright flame spot observed close to the LOX post tip suggests that a well-mixed flame with strong radiation was anchored in an intensive recirculation zone. This could be observed over the entire range of test conditions, for injectors with and without recess, and for a LOX post tip thickness of only 0.3 mm. The well-mixed flame then functioned as a flameholder for the rest of the flame. The LOX post wake could be tracked at least 15 LOX jet diameters downstream and significantly influenced the layer of reacting gases.

The influence of H_2 injection temperature on mixing performance near the injector was also studied over the temperature range of 150–300 K. Two chamber pressures of 6.0 and 10.0 MPa were selected for comparison, with O_2 and H_2 injection velocities kept constant at 30 and 300 m/s, respectively. Because of the marginal, though not exactly known, value of the surface tension, the Weber number did not seem to be an appropriate parameter to characterize the mixing process. Assuming mixing is controlled by the momentum ratio, and assuming this was controlled by the fuel stagnation pressure because the LOX momentum was almost constant in this study, it was expected that a decreased H_2 injection temperature would lead to an increased H_2 density that would intensify the mixing process. However, varying H_2 temperature affected mixing to a smaller extent than the overall chamber pressure. Increasing the chamber pressure also increases the H_2 density, and this turned out to have a larger effect on mixing than the H_2 temperature. Futher details of this study may be found in Mayer and Tamura.[3]

Cold-Flow Jet Studies

Although lacking the realism of combustion, cold-flow studies provide the opportunity to visualize atomization and breakup processes without the optical distortions that combustion introduces. Cold-flow studies have been performed at full scale,[4] where injector sizes and flow rates are similar to those in actual applications, and also using smaller, subscale elements and flows.[5] Recent results are summarized next.

Fig. 4 Burning LOX jet at a supercritical pressure of 6.0 MPa (test case 3). Axial positions are x = 0 (faceplate), 12, 24, 36, 48, and 60 mm, from left to right and top to bottom.[3]

Full-Scale Studies

LN_2 and GH_2 or gaseous helium (GHe) were used as simulants in cold-flow studies using the test apparatus illustrated in Fig. 6.[4] The pressure was kept constant (up to 6.0 MPa), independent of the injected mass flow. The temperatures of the injected fluids were measured close to the injector exit. The LN_2 injection temperatures reached as low as 90 K, whereas the GHe and GH_2 temperatures ranged between 100 and 370 K. The study covered a range of injection conditions and injector geometries. Quantitative measurements of time and length scales were obtained using flashlight photography and high-speed cinematography (30 kHz), and qualitative measurements of species distributions were obtained using Raman spectroscopy. Flow regimes were expressed in terms of appropriate dimensionless numbers such as the Weber number ($We = u_{rel}^2 \rho_g D_{jet}/\sigma$), and liquid and gas Reynolds numbers.

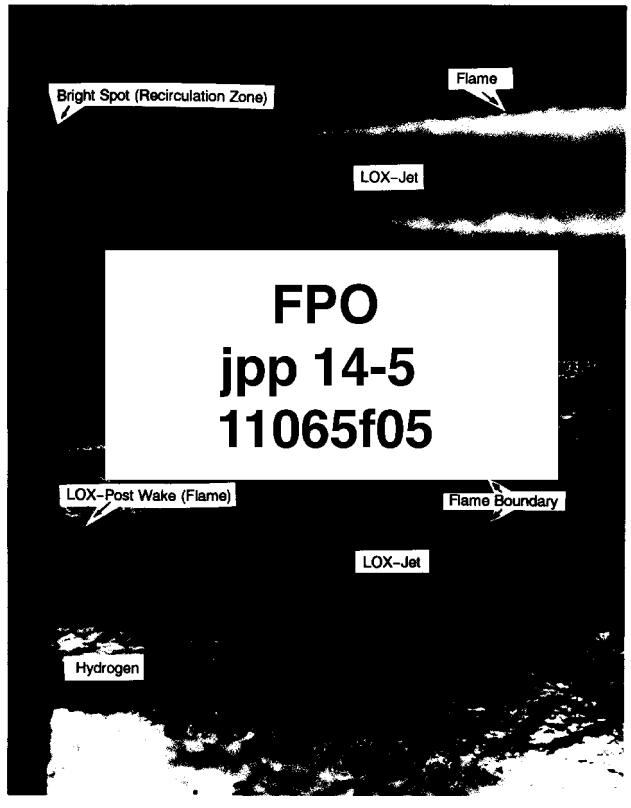

Fig. 5 Near injector region for a supercritical pressure of 4.5 MPa (test case 2): a) Flame and b) corresponding flowfield.[3]

Figure 7 shows the injection of LN_2 at 97 K with coaxially flowing helium (He) at 280 K into GHe at 300 K, at backpressures of 1.0 and 6.0 MPa. In this figure, the LN_2 injection velocity was 10 m/s, the GHe velocity was 100 m/s, the initial LN_2 diameter was 1.9 mm, and the GHe annular gap thickness was 0.2 mm. The formation of ligaments and the detachment of droplets from them can be seen at 1.0 MPa, but not at 6.0 MPa. Mixing in the latter case is more like that between a dense and a light fluid in a turbulent shear layer. At Reynolds numbers exceeding 1×10^4 and for pressures higher than 70% of the critical pressure, the structure of the interface was dominated by turbulence at reduced surface tension, and did not depend on whether the pressure was supercritical or subcritical.

Figure 8 shows injection behavior in a pure N_2 system in the absence of He, where mixture effects on the critical properties are absent. LN_2 was injected at 105 K and a velocity of 1 m/s into warm N_2 at 300 K at chamber pressures of 2.0, 3.0, and 4.0 MPa. The injector diameter was 1.9 mm. At the subcritical pressure of 2.0 MPa, the jet surface is smooth and clearly identified with large-scale disturbances. At 3.0 MPa, which is 0.4 MPa below the critical pressure, the jet looks quite different. Because of the reduced surface tension, small-scale turbulent structures are able to disturb the interface and even leave the jet in the form of droplets. At the supercritical pressure of 4.0 MPa, the surface changes into a streaky interface. The cross section of the jet increases with the downstream distance like a gaseous jet. The state of the injected N_2 changes from a liquid to a dense fluid with rising pressure. The atomization mechanism seems to change considerably in the absence of surface tension. As ambient pressure is increased with surface tension present, the length scales of breakup (ligament and droplet diameters) decrease. As surface tension drops further below a certain limit, the atomization mechanism changes to one of a shear-layer instability. Observable length scales become larger.

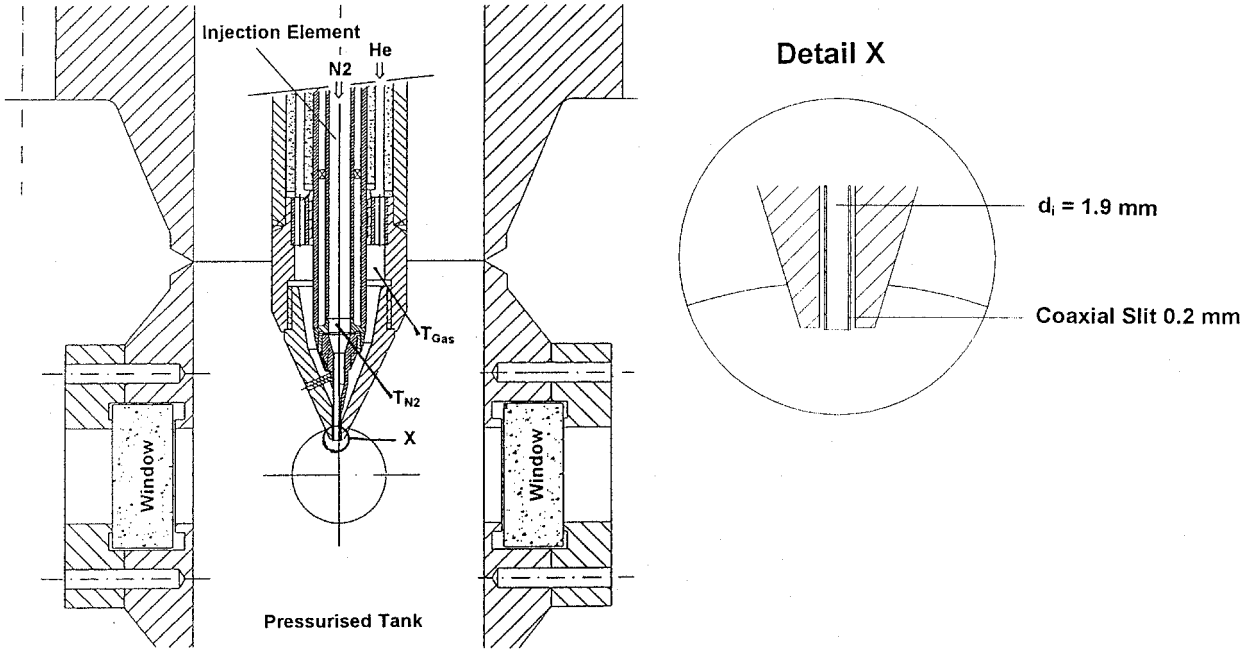

Fig. 6 Test chamber for full-scale cold-flow studies.

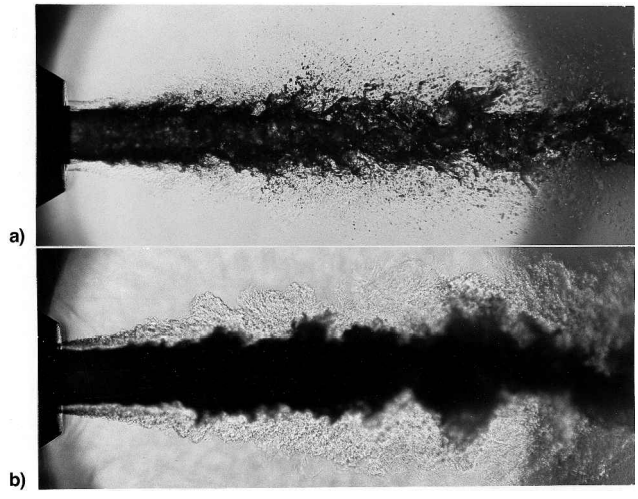

Fig. 7 Coaxial LN_2/GHe injection at a) 1.0 and b) 6.0 MPa.

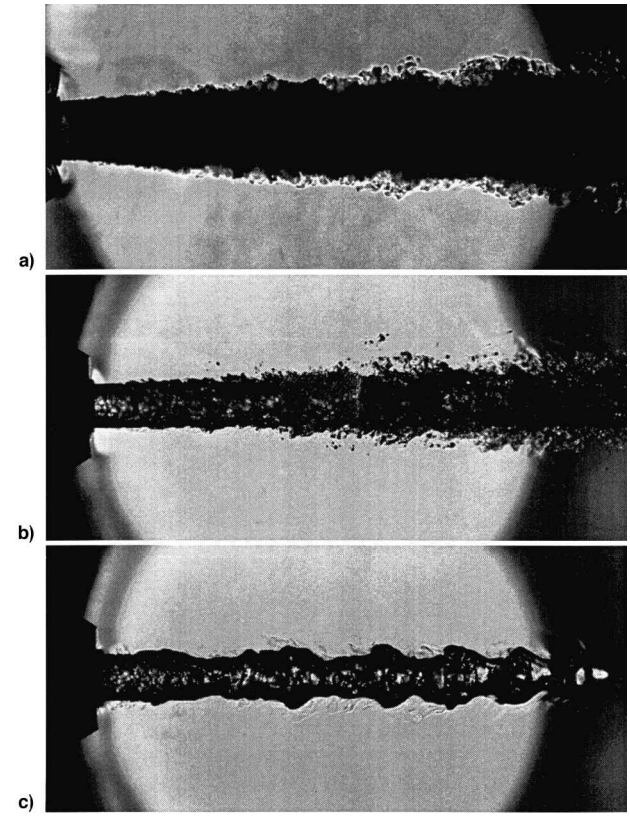

Fig. 8 LN_2 injection into GN_2 at a) 4.0, b) 3.0, and c) 2.0 MPa.

Subscale Studies

Subscale cold-flow studies with smaller injector dimensions than in actual applications have been performed to further reduce optical distortions and better resolve the details of the fluid interfaces.[5] Experimental results for subscale round LN_2 jets injected into GHe/GN_2 mixtures are shown in Fig. 9 at various pressures for an injector diameter of 0.25 mm, a LN_2 temperature of 90 K, a chamber temperature of 250 K, and an injection velocity of 1.3 m/s. In Fig. 9 the horizontal rows (1)–(3) correspond to different axial locations in this figure, whereas the vertical columns (9a–9d) correspond to different experimental conditions. Shadowgraph images of LN_2 jets into pure GN_2 are shown in Figs. 9a–c, for subcritical (Fig. 9a), near critical (Fig. 9b), and supercritical (Fig. 9c) pressures. The effect of pressure (and thus fluid state) on mixing is quite drastic, with jets in Figs. 9b and 9c exhibiting a laminar liquid-like appearance near the orifice and a turbulent gas-like appearance farther downstream. A small sheet of fluid can be seen emanating from the side of the jet in Fig. 9b (row 1) and 9c (row 1) as a result of a small imperfection in the orifice, but the sheet is not present in Fig. 9a (row 1). Surface tension is evidently large enough to prevent the formation of this sheet at the subcritical pressures in Fig. 9a (row 1), whereas it is not sufficient to do so at the near- and supercritical pressures Figs. 9b (row 1) and 9c (row 1). This is despite the fact that density gradients at the interface in Fig. 9b (row 1) and Fig. 9c (row 1) remain large enough to cause a liquid-like appearance. For Fig. 9d, the pressure was kept at twice the critical pressure of pure N_2, as in Fig. 9c, but He was added to the ambient in 9d to a GN_2/GHe ratio of 3.9 by mass. Liquid-like structures exhibiting evidence of surface tension are shown to be recovered because of the mixture effects involved in adding He.

Figure 10 depicts another series of shadowgraph images of LN_2 jets injected this time into GHe at chamber pressures of 5.5, 6.9, and 8.3 MPa. The jet velocity was 1.7 m/s, the LN_2 temperature was 83 K, and the chamber temperature was 292 K. In Fig. 10b, surface tension apparently still dominates the jet breakup dynamics. After initial jet breakup, no spherical structures are formed. Unsteady aerodynamic forces cause many irregular shapes as interfacial tension is too weak to reshape the fluid into spheres. Figure 10c reveals a marked change in the nature of the jet structure. Although what appear to be interfacial features continue to be observed, any remnants of surface tension playing a role in the jet disintegration appear to have vanished. Injection under these latter conditions is seemingly more characteristic of a turbulent, viscous gas jet. Jet structure is characterized by wispy structures barely, if at all, retained by interfacial forces. Thin threads of fluid, undisturbed by surface tension forces, are able to connect larger blobs until aerodynamic forces perturb them. Consistently, no structures suggestive of surface discontinuities are observed downstream of position 2, indicating an advanced state of mixing, though not necessarily complete. Surface tension apparently ceases to be important in the jet disintegration process somewhere between 5.5 and 6.9 MPa (1.6–2.1 times the critical pressure of pure N_2), for the particular conditions of this N_2/He system, as witnessed in the upper part of the jet. However, one might question why the LN_2 jet in Fig. 9d, injected into the N_2/He mixture at 6.9 MPa, exhibits jet behavior indicative of a subcritical liquid state, whereas the jet in Fig. 10b in pure He at the same pressure exhibits behavior indicative of a supercritical state. The answer is probably related to the relatively small differences in jet and ambient temperatures and jet velocities. Figure 11 depicts a LN_2 jet injected into He at the low-pressure end of this transition range, 5.5 MPa. Jet and ambient conditions are the same as in Fig. 10b. In this sequence of images recorded at identical injection conditions, an oscillation between gas-like and liquid-like jet behavior can be seen. These examples illustrate that under certain conditions the nature of the jet breakup process can be extremely sensitive to small perturbations in pressure, temperature, local mixture concentrations, and initial jet conditions. In application, the oscillation in the jet breakup behavior could lead to local propellant mixture ratio oscillations and conceivably unstable combustion behavior.

Single Droplet Studies

Single droplet processes provide even more opportunity to clearly visualize simple flows and are themselves important processes in combustion. Studies of single cryogenic droplets at high pressures have been undertaken under both subcritical[9,10] and transcritical conditions. The transcritical results are reported herein for the first time.

High-Pressure Subcritical Droplet Studies

Breakup regimes of subcritical cryogenic LOX droplets subject to aerodynamic shear forces were investigated for various

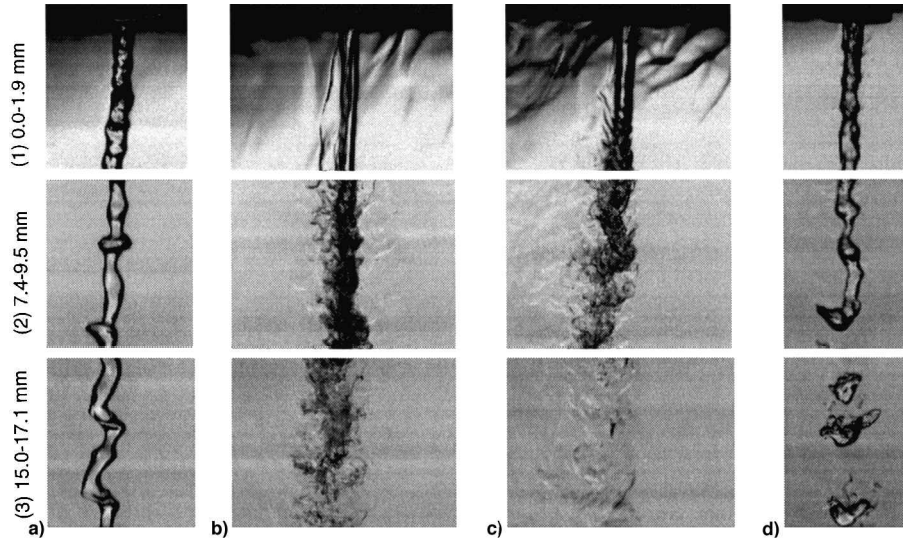

Fig. 9 Subscale LN_2 injection into a pressurized chamber. Horizontal rows correspond to distance from the injector tip. Vertical columns correspond to different experimental conditions as follows: a) Into subcritical N_2 at 2.8 MPa, $p/p_{crit} = 0.83$; b) into near critical N_2 at 3.5 MPa, $p/p_{crit} = 1.03$; c) into supercritical N_2 at 6.9 MPa, $p/p_{crit} = 2.03$; and d) into a $N_2/O_2 = 3.9$ mixture at 6.9 MPa, $p/p_{crit} = 2.03$.

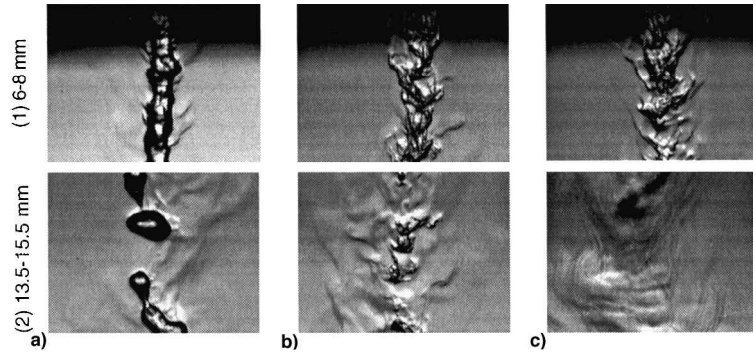

Fig. 10 LN_2 jets injected into He at elevated pressures.

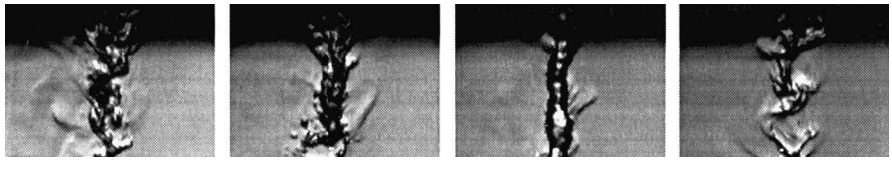

Fig. 11 Image sequence of LN_2 jets injected into He at 5.5 MPa reveals oscillation between liquid-like and gas-like behavior.

droplet Reynolds numbers, Weber numbers, and liquid-to-gas density ratios.[9] Single droplets were vertically injected into the potential core region of a horizontal 300-K dry airjet in a pressure vessel capable of sustaining pressures up to 12.0 MPa. This allowed for the investigation of droplet behavior at lower density ratios than has previously ever been examined. Flow and turbulence characteristics of the jet were determined by two-component laser Doppler anemometry, and the droplets were visualized using rapid video imaging and numerical image analysis.

LOX droplets with diameters between 600 μm and 1.0 mm were studied over a pressure range of 0.1–4.0 MPa for jet velocities ranging from 0.4 to 86 m/s. The corresponding maximum values of the droplet Weber number ($We = u_{rel}^2 \rho_g D/\sigma$), Reynolds number ($Re = \rho_g u_{rel} D/\mu_g$), and Ohnesorge number [$Oh = \mu_g/(\rho_g D\sigma)^{1/2}$] were 800, 7500, and 0.01, respectively. The liquid-to-gas density ratio varied between 20 and 1040. The surface tension changed significantly over this pressure range, decreasing from 13.6×10^{-3} N/m at 0.1 MPa to 4.97×10^{-3} N/m at 3.0 MPa. The enthalpy of vaporization also decreased significantly as pressure increased, which reduced global gasification times. Four droplet-jet interaction regimes are illustrated in Fig. 12 corresponding to deformation, bag, transitional, and shear breakup regimes.

To better isolate the effects of vaporization and reduced surface tension from the effect of changing density ratio, ethanol droplets were also studied (see Table 1). The ethanol droplets vaporized much more slowly than the LOX droplets, and the surface tension changed by only about 10%, from 22.8×10^{-3} at 0.1 MPa to 20.0×10^{-3} at 3.0 MPa. In the ethanol experiments, the pressure was varied from 0.1 to 5.0 MPa, and the corresponding liquid-to-gas density ratio varied between 16 and 800. The maximum droplet Weber number was 90, and the maximum droplet Reynolds number was 1.6×10^4. The droplet Ohnesorge number was less than 0.02 for all cases. The diameters of ethanol droplets were kept at 600 μm.

A comparison between the results obtained for the ethanol and LOX experiments is presented in Fig. 13 for a pressure of 3.0 MPa. Transition droplet Reynolds numbers are observed to be much higher for the ethanol droplets. For example, the shear breakup regime was attained at a droplet Reynolds number of 4×10^3 for LOX droplets but at a droplet Reynolds number of 1.2×10^4 for the ethanol droplets. Because of the reduced surface tension of the LOX, the same droplet Reyn-

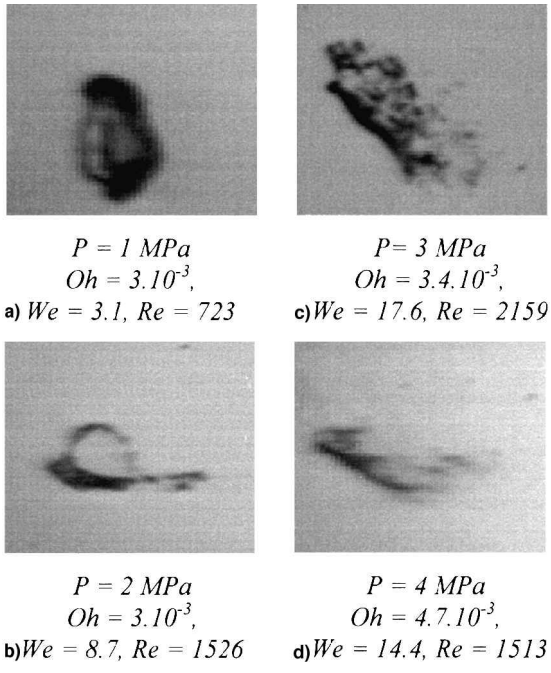

Fig. 12 Droplet breakup regimes for LOX droplets: a) Deformation, b) bag, c) transitional, and d) shear.

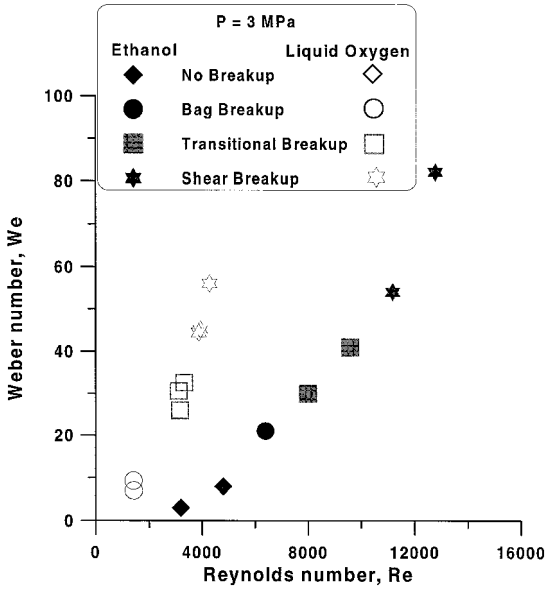

Fig. 13 Comparison of the deformation and breakup regimes between ethanol and LOX droplets.

olds numbers produce higher droplet Weber numbers than the ethanol droplets. As a result, higher breakup regimes are attained with smaller aerodynamic forces. It is important to note that the variations in droplet Reynolds numbers in Fig. 13 were obtained entirely by varying the airjet velocity. All other physical parameters remained constant, including densities, droplet diameter, and dynamic viscosity.

Breakup initiation times were another important feature that was determined for LOX droplets at various pressures. Experimental initiation and total breakup times, normalized by $(D/V)(\rho_l/\rho_g)^{1/2}$, are shown in Fig. 14 for LOX droplets at 4.0 MPa. The breakup initiation time was defined as the time delay between the exposure of the droplet to the aerodynamic shear forces and the first clear observation of the corresponding breakup regime (bag, transitional, or shear). The total breakup time was defined as the time delay from the entry of the droplet into the airjet to the end of the deformation and breakup processes undergone by all of the droplets.[10] As shown in Fig. 14, total breakup times increased with Weber number, but initiation times decreased. These opposite trends mean that drop deformation and breakup occur sooner but last longer as the Weber number is increased.

Transcritical Droplet Studies

A unique droplet generator for producing transcritical LOX and LN_2 droplets was constructed. The generator was mounted in a 13.7-MPa pressure vessel having two 133.4-mm sapphire windows for observation. High-pressure gaseous O_2 or N_2 was condensed in a central tube by an atmospheric pressure LN_2 bath. A piezoelectric crystal inside the tube provides acoustic excitation for forming the droplets. The droplets are created in a flow of GHe chilled to the same temperature as the droplets. The He provides a molecular weight difference to provide a surface for forming the droplets. The helium flows through a converging–diverging section with the drop generator located near the throat. This allows aerodynamic stripping to also be used to produce droplets. In the pressure vessel, He forms a buoyant layer and the droplets fall into warm test gas of interest, for example, N_2/He mixtures.

A representative shadowgraph of the results is given in Fig. 15. LOX droplets having an initial temperature of 177 K were produced in a chilled helium coflow of about the same temperature and fell into a pure GN_2 gas at a pressure of 6.6 MPa and a temperature of 290 K. N_2 gas was used in the pressure vessel instead of O_2 gas for safety reasons and because N_2 has very little effect on the critical properties of O_2. The increasing panel numbers in Fig. 15 correspond to increasing distances downstream. The 0.254-mm wire visible in panel 1 was in-

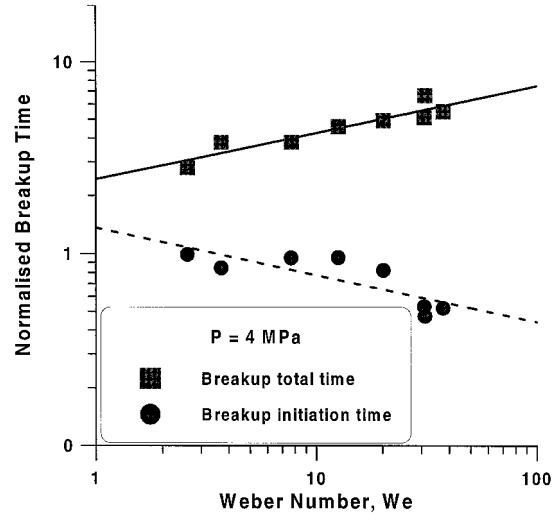

Fig. 14 Comparison between breakup initiation and total breakup times at 4.0 MPa for LOX droplets.

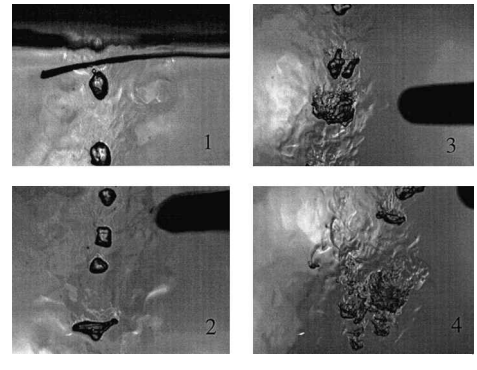

Fig. 15 Transcritical LOX droplets falling into GN_2. Increasing panel numbers correspond to increasing distances downstream.

serted behind the droplet stream as a size reference and also to provide an indication of the degree of optical distortion. Panel 1, which exhibited very low distortion, provides a good indication of the shape of the reference wire, which was not straight. The dark shadows visible in the images are 1.6-mm thermocouples. A buoyant He layer was formed at the top of the pressure vessel that extends just below the bottom of panel 1. The fluids seen in panels 2–4 are largely N_2 and O_2. A slow N_2 "wind" is flowing from right to left in these images. Thus, the smooth gray areas to the right of the panels are N_2 and the lighter-colored turbulent areas to the left are in the droplets' wake and are N_2/O_2 mixtures.

Quantitative results have not yet been obtained, but qualitatively it was observed that the droplets exhibited no resistance to deformation and, therefore, no evidence of surface tension once they dropped below the He layer. An inverse bag shape can be seen in panel 2, and in panel 4 such shapes are seen to be joined by "tails" in a mushroom shape that are often observed. Various-sized globs of fluid break off at unpredictable times and spread, contributing to the mixing. Cellular structures can be observed in panel 3, but it is unclear whether this is because of an instability or simply a response to turbulence. Further efforts are underway to quantify these effects as a function of various parameters.

Summary and Conclusions

Recent results on the atomization and breakup of cryogenic propellants under high-pressure subcritical and supercritical conditions have been reviewed. The work ranged from studies of the principal character of coaxial flow to detailed investigations of ligament and drop breakup and mixing.

All of the experiments show that as pressure is increased, fluids eventually reach a transcritical regime where breakup and mixing are no longer influenced by surface tension. Subsequently, the fluids behave more like viscous miscible fluids. The pressure at which the transition occurs is a strong function of the ambient composition and initial conditions, and cannot be deduced from the critical pressure of the pure species alone. Strong convection effects may make precise identification of the transition pressure impossible.

The hot-fire tests revealed that a flame was always attached to the LOX post, and the interface between the propellants is separated by a layer of hot reacting gas. At very low pressures, the LOX jet exhibits a smooth surface and breaks up into a small number of nonspherical droplets that evaporate rapidly. At transcritical pressures the LOX jet develops stringy fluid structures that rapidly dissolve. Further downstream the jet develops nonaxisymmetric snake-like oscillations of growing amplitude until it breaks up. Large lumps of O_2 were visualized several tens of jet diameters downstream. This "heavy mixing zone" is characterized by large-scale turbulence, maximum amplitudes of O_2 jet oscillations, a slight widening of the O_2 jet and of the flame, dispersion of the O_2 ligaments, and the strongest combustion radiation.

Studies of LOX droplet breakup under high-pressure subcritical conditions near the critical pressure show that breakup initiation times decrease but that the total breakup time increases as the droplet Weber number increases. A comparison between the LOX droplets and ethanol droplets under similar conditions, where the LOX droplets had lower surface tension than the ethanol droplets, showed that transition to higher breakup regimes occur at larger droplet Reynolds numbers for the enthanol droplets. As pressures increase into a transcritical regime, no indication of surface tension was found and the droplets were incapable of resisting deformation. Random clumps of fluid broke off at unpredictable times, which may enhance the mixing.

Acknowledgments

The work done at DLR Lampoldshausen was supported by Deutsche Agentur für Raumfahrtangelegenheiten; the work at the U.S. Air Force Research Laboratory was supported by the U.S. Air Force Office of Scientific Research; and the work at Laboratoire de Combustion et Systèmes Réactifs, Orleans, France was supported by the joint CNRS/CNES/SEP program on Combustion in Cryogenic Rocket Motors.

References

[1]Immich, H., and Mayer, W., "Cryogenic Liquid Rocket Engine Technology Developments Within the German National Technology Programme," AIAA Paper 97-2822, July 1997.

[2]Mayer, W., "Coaxial Atomization of a Round Liquid Jet in a High-Speed Gas Stream: a Phenomenological Study," *Journal of Experiments in Fluids*, Vol. 16, No. 6, 1994, pp. 401–410.

[3]Mayer, W., and Tamura, H., "Propellant Injection in a Liquid Oxygen/Gaseous Hydrogen Rocket Engine," *Journal of Propulsion and Power*, Vol. 12, No. 6, 1996, pp. 1137–1147.

[4]Mayer, W., Schik, A., Schweitzer, C., and Schäffler, M., "Injection and Mixing Processes in High-Pressure LOX/GH2 Rocket Combustors," AIAA Paper 96-2620, 1996.

[5]Woodward, R. D., and Talley, D. G., "Raman Imaging of Transcritical Cryogenic Propellants," AIAA Paper 96-0468, 1996.

[6]Yang, V., Lin, N. N., and Shuen, J. S., "Vaporization of Liquid Oxygen (LOX) Droplets in Supercritical Hydrogen Environments," *Combustion Science and Technology*, Vol. 97, 1994, pp. 247–270.

[7]Delplanque, J.-P., and Sirignano, W. A., "Numerical Study of the Transient Vaporization of an Oxygen Droplet at Sub- and Supercritical Conditions," *International Journal of Heat and Mass Transfer*, Vol. 36, 1993, pp. 303–314.

[8]Oefelein, J. C., and Yang, V., "Simulation and Analysis of Supercritical Multiphase Combustion Processes," AIAA Paper 96-2880, 1996.

[9]Chesneau, X., Chauveau, C., and Gökalp, I., "Experiments on High-Pressure Vaporization of Liquid Oxygen Droplets," AIAA Paper 94-0688, 1994.

[10]Vieille, B., Chauveau, C., and Gökalp, I., "Droplet Breakup Regimes Under High-pressure Conditions," *Proceedings of the 13th Annual Conference on Liquid Atomization and Spray Systems* (Florence, Italy), 1997, pp. 195–201.

[11]Vieille, B., Chauveau, C., and Gökalp, I., "Droplet Break-Up Regimes of LOX Droplets Under High-pressure Conditions," AIAA Paper 98-0715, Jan. 1998.

[12]Anderson, T., Woodward, R. D., and Winter, M., "Oxygen Concentration Measurements in a High-pressure Helium Environment Using Raman Imaging," AIAA Paper 95-0140, Jan. 1995.

Color reproductions courtesy of DLR, German Aerospace Research Center.